International Journal of Mechanical, Industrial and Aerospace Sciences
ISSN: 2517-9950
Vol:3, No:12, 2009

Accurate Dimensional Measurement of 3D Round Holes Based on Stereo Vision

Zhiguo Ren, Lilong Cai

Abstract**—**This paper present an effective method to accurately reconstruct and measure the 3D curve edges of small industrial parts based on stereo vision. To effectively fit the curve of the measured parts using a series of line segments in the images, a strategy from coarse to fine is employed based on multi-scale curve fitting. After reconstructing the 3D curve of a hole through a curved surface, its axis is adjusted so that it is parallel to the *Z* axis with least squares error and the dimensions of the hole can be calculated on the *XY* plane easily. Experimental results show that the presented method can accurately measure the dimensions of round holes through a curved surface.

Keywords**—**Stereo Vision, 3D Round Hole Measurement, Curve Fitting, 3D Curve Reconstruction, Least Squares Error.

I. Introduction

ACCURATE measurement plays an extremely important role in modern manufacturing processes. Due to the inherent manufacturing errors of industrial parts, a high level of the measurement accuracy should be adopted at the important stages of a manufacturing process to guarantee strict dimensional tolerances. Traditional precise measurement methods are often based on high-skilled personnel who perform a series of measurements using special measurement instruments such as gauges, micrometers, etc. However, manual measurement methods often have a number of drawbacks like prone to human errors, low efficiency and high cost. Therefore, to develop automatic precise 3D measurement methods is becoming a challenging research topic[1] .

Most industrial parts can be represented by line frames, including line segments, circles, arcs, ellipses and general curves. However, linear distances, angles and diameters of round holes are always the most measured dimensions in most industrial measurements of accurate parts. Although much investigation has been carried out on the automatic measurement of circles or ellipses on a plane[2], the measurement of round holes through curved surfaces is often a challenging issue.

Typical 3D measurement technologies mainly include contact measurement methods like coordinate measuring machines (CMMs)[3], and non-contact measurement methods such as laser scanning[4, 5], structured light[6], and photogrammetry methods[7].

Zhiguo Ren and Lilong Cai are with the Department of Mechanical Engineering, Hong Kong University of Science and Technology, Clear Water Bay, Kowloon, Hong Kong. (e-mail:renzg@ust.hk)

Although these automatic 3D measurement methods have been applied in industrial manufacturing processes, there are still several obstacles associated with these methods. Special 3D round holes often appear in complicated small industrial parts, and most of these methods, such as CMMs, laser scanning and structured light, can not be directly adopted, especial for some small parts. However, stereo vision may be a feasible technique for the 3D measurement of these small parts, and the method has been widely applied to 3D measurement.

To effectively reach automatic measurement, prior knowledge of the measured parts by means of CAD models is often exploited. In automatic measurement, the initial estimation of the measured features can be determined by the CAD model and the calibration of a stereo vision system. Curve feature extraction is a difficult task in image processing and stereo vision. For some special curves, such as circles and ellipses, which can be represented by a set of parameters, the standard HT (Hough Transform) method is often adopted [8]. For some projections of complicated 3D curves, they are often difficult to represent using simple parameters. In fact, these curves can be represented by a series of pieces of conics [2, 9-12]. However, although these methods using conic pieces can accurately represent various curves, they are often complicated and involve a large amount computation. Alternatively, many techniques have been proposed by using short linear segments to approximately represent various curves in investigation [13, 14].

Line fitting is an important method in detecting linear features in images. By estimating and canceling noise, some line fitting methods can exactly extract the desired linear features [15, 16]. In addition, least squares linear template matching has also been used in linear feature extraction [17]. Some of these linear feature extraction methods have been applied in practical measurements of general artificial objects. However, in real automatic measurement processes, the measured small parts often can not be located accurately in a product line due to the errors of the fixture. That will lead to large errors of the initial estimation of the position and pose of the measured parts. Thus, even with the prior knowledge of the CAD models, these linear feature extraction methods often fail to extract the exact line pieces to represent the desired curves.

To reconstruct a 3D curve by using the extracted curves in two images is another key task. The epipolar method is one of the most important methods of 3D reconstruction based on stereo vision. It describes the inherent geometric relationships between 3D points of a scene and their projections in the images acquired by two or more cameras. This method has been investigated and applied widely [18], and is feasible to be

adopted to reconstruct the measured 3D curve.

In this paper, an effective method to reconstruct and measure the dimensions of 3D round holes through curved surfaces is proposed. Using a strategy from coarse to fine, the desired curves can be accurately fitted by a series of line segments in a complicated background. Furthermore, according to the obtained curve features, the 3D curve of the hole can be reconstructed by using the epipolar line method. Then, the desired dimensions of the 3D holes can be accurately calculated by adjusting its axis so that it is parallel to the *Z* axis. Our experimental results show that the presented method can accurately measure the diameters of 3D round holes through curved surfaces in small parts.

The paper is organized as follows. Section 2 introduces the representation of 2D curves. Section 3 presents an effective method for curve fitting. In Sections 4, after introducing the 3D reconstruction method, a method for round hole measurement is represented. Section 5 reports the experimental results to verify the proposed method. The last section summarizes the method and offer the conclusions.

II. Curve Representation

As some real curves are difficult to be represented by using simple parameters, they are often represented by a series of circular arcs, conic sections, or short straight lines. However, using a series of connected line segments to represent a curve is a simple and effective method. Fig. 1 shows a curve that can be represented by a series of line segments, P_1P_2, P_2P_3, …, $P_iP_{(i+1)}$.

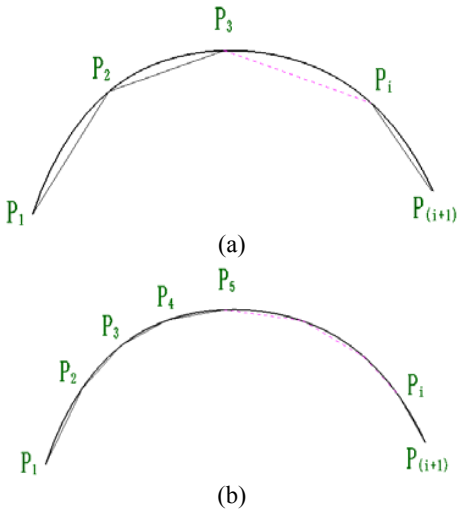

Fig. 1 Represent a curve using a series of line segments, (a) using a series of long line segments; (b) using a series of short line segments.

In 2D images, a curve can be fitted by a series of connected line segments, and every line segment fits a section of the curve. Generally, a long line segment can fit a section of curve with strong robustness but gives larger errors. On the other hand, a short line segment can fit a section of the curve with a high accuracy, but is sensitive to the noise in the background. Therefore, a multi-scale representation method to fit the desired curves from coarse to fine in images is proposed.

III. Curve Fitting Using Virtual Beam Chains at Multi-Scales

To effectively extract the desired curve features in an image, a method combining the local gradient information and the global topological structure of the desired curve features from coarse to fine is proposed. Based on a virtual system, the problem of how to extract the curve feature in an image can be transformed into a virtual motion process. The virtual system is composed of a virtual beam chain at different scales, and a virtual attraction field. In the virtual attraction field, all the beams can be attracted, and move towards the strong attraction source. When the resultant force on the virtual beam chain is zero, it will stop moving. Thus, the beam chains will effectively fit the desired curve.

Depending on the CAD model of the measured part and the calibration of the stereo vision, the initial estimation of the projection of the 3D curve can be calculated. As the curve is represented by a series of line pieces, the line pieces can be considered as a virtual beam chain that is built by a series of virtual beams connected by virtual joints (shown in Fig. 2). In the virtual beam chain, every beam represents a fitting line for a section of the curve. All the virtual joints can be notated by P_i ($i = 1,2,...,n$). Each beam has two joint holes at its ends, and is connected with adjoining beams. When these beams are subjected to an external force, an assumption that they can be stretched or compressed without bending can be made.

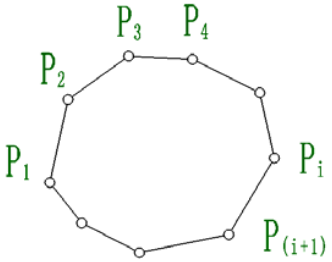

Fig. 2 A virtual beam chain

Using the gradient along the direction perpendicular to the corresponding virtual beam, a virtual attraction field in which every pixel is a virtual attraction source can be built. The intensity of the virtual attraction source is defined by

$$A(X,Y) = \left|\nabla I(X,Y)\sin[\gamma(X,Y) - \beta]\right|, \quad (1)$$

where $\nabla I(X,Y)$ denotes the gradient modulus in the gray image $I(X,Y)$. $\gamma(X,Y)$ is the angle of the gradient direction in (X,Y), and β is the angle of the direction of the corresponding virtual beam.

When the virtual beam chain is put into the virtual attraction field according to the initial position estimation, all the beams will be attracted by the virtual attraction sources. To ensure the effectiveness of the virtual system, the attraction sources are limited in a valid range beside each beam, in which the perpendicular distance from the valid attraction source to the beam is limited by *W*.

In the virtual system, it is required that the attraction is perpendicular to the beams and is in direct proportion to the intensity of the virtual attraction source described in equation (1). This rule ensures that the beams can converge to the desired curve in which there is a strong intensity of attraction. In addition, it is assumed that the attraction is in direct proportion to the perpendicular distance from the attraction source to the beam like a spring system. This assumed rule can drive the beams to quickly move towards objects in remote positions.

In the virtual model, a local frame, *oxy*, on a virtual beam (shown in Fig. 3) is built. Then, the subjected attraction distribution on every beam is represented by

$$\mathbf{f}_i(x) = A(x_j, y_j)\mathbf{D}(x_j, y_j), \tag{2}$$

where $\mathbf{D}(x, y)$ denotes the perpendicular vector from the attraction source in (x_i, y_i) to the beam. A schematic depicting of the attraction distribution on a beam (P_i, $P_{(i+1)}$) is shown in Fig. 3.

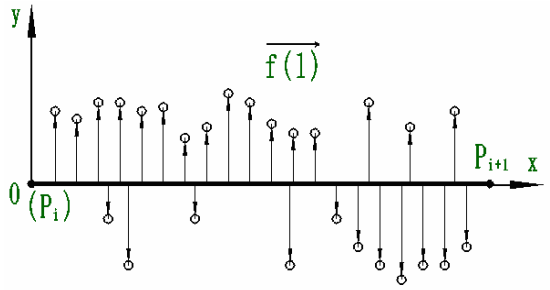

Fig. 3. Schematic attraction distribution on a beam

According to the principle of structural mechanics, the distribution of attraction on each beam can be transformed into a couple of equivalent forces on the two end points of the beam by

$$\begin{cases} \mathbf{F}_{i+} = \dfrac{1}{L}\sum_{j=1}^{j=n}\mathbf{f}(x)(L-x) \\ \mathbf{F}_{(i+1)-} = \dfrac{1}{L}\sum_{j=1}^{j=n}\mathbf{f}(x)x \end{cases}, \tag{3}$$

where L is the length of the beam. Using the same method, each couple of equivalent forces on the end points of all the beams can be calculated.

As in the local frame, the value of $\mathbf{D}(x, y)$ can be represented by y, the equivalent forces on the two end points of the beam are finally represented by

$$\begin{cases} \mathbf{F}_{i+} = \dfrac{1}{L}\sum_{j=1}^{j=n}A(x,y)y(L-x) \\ \mathbf{F}_{(i+1)-} = \dfrac{1}{L}\sum_{j=1}^{j=n}A(x,y)yx \end{cases}. \tag{4}$$

If a virtual joint (P_i) has a small displacement $[\Delta X_i, \Delta Y_i]$ from (P'_i) in the world coordinate system, shown in Fig. 4, the equivalent forces at the end points of the beam can be calculated according to equation (4). Ignoring the high-order terms and the change of the length of the beam, the equivalent force at the end point (P_j) of the beam (P_i, $P_{(i+1)}$) is represented by

$$\mathbf{F}_{i+} = \frac{1}{L}\sum_{j=1}^{n}A(x,y)(y - \frac{L-x}{L}\Delta y)(L-x). \tag{5}$$

According to the coordinate transformation from the local frame to the world coordinate system, the following relationship can be gotten.

$$\Delta y = -\Delta X_i \sin\beta_{ij} + \Delta Y_i \cos\beta_{ij}, \tag{6}$$

where β_{ij} is the angle of the direction of the beam. Combining equation and (6), the equation (5) can be rewritten as

$$\begin{aligned} \mathbf{F}_{i+} &= \frac{1}{L}\sum_{j=1}^{n}A(x,y)y(L-x) \\ &+ \frac{(\Delta X_i \sin\beta_{ij} - \Delta Y_i \cos\beta_{ij})}{L^2}\sum_{j=1}^{n}A(x,y)(L-x)^2 \end{aligned}. \tag{7}$$

Using the same method, the equivalent force on every end point of the beams connected by the virtual joint (P_i) can be calculated.

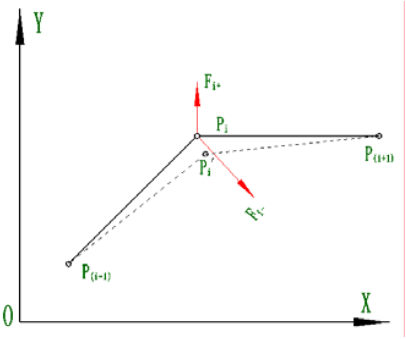

Fig. 4. The schematic force status on joint (P_i)

Since a virtual joint usually connects two adjoining beams, the resultant force on the virtual joint (P_i) can be calculated by

$$\mathbf{F}_i = \mathbf{F}_{i+} + \mathbf{F}_{(i+1)-}, \tag{8}$$

where $\mathbf{F}_{i+}$ and $\mathbf{F}_{(i+1)-}$ are the equivalent forces on each end point of the adjoining beams.

When the joint (P_i) reaches a force balance, according to equation (8), it can be described by

$$\mathbf{F}_{i+} + \mathbf{F}_{(i+1)-} = 0. \tag{9}$$

By resolving the vector equation, the solutions of the displacement $[\Delta X_i, \Delta Y_i]$ in equation (7) can be figured out. Furthermore, using the same method, the desired displacement on every joint can be obtained. When the force on every joint reaches zero, the beam chain can fit the desired curve.

As there are often large errors in the initial estimated positions of the beam chain due to the inaccurate fixture and installation of the measured parts, the original beam chain, $P_1, P_2, P_3, ..., P_N$, (with longer beams) is first used to fit the curve. Then, the beam chain is decomposed into $1/2$ scale by splitting every virtual beam into two equal halves, and all the virtual joints can be represented

by $P_1, P_2, P_3, ..., P_N, P_{N+1}, ..., P_{2N}$. Inheriting the previous fitting results and using the obtained beam chain at a smaller scale, the desired curve can be continuously fitted with a higher accuracy. Repeating the beam decomposition and fitting process, the desired curve can be extracted from coarse to fine at different scales, such as $1/2, 1/4, ..., 1/2^S$, where *S* is the scale index.

IV. Three-dimensional Curve Reconstruction and Measurement

Using the features of the curves in two images acquired by our stereo vision system, one of the effective methods to reconstruct the 3D curve is the epipolar line method. Fig. 5 shows the principle. S_1 and S_2 are the projection points of the left and right CCDs, respectively. *P* is an arbitrary point of a 3D curve, *C*, in the space, and its two corresponding projection points in the two images are denoted by *p* and *p'*. According to the projection relationship in the vision system, the points, *P*, *p*, *p'*, S_1 and S_2 are coplanar. The coplane can be denoted by Π. Thus, for the given point *p* in the left image, the corresponding *p'* in the right image is constrained to lie on the epipolar line of *P*, which is the intersection of plane Π and the right image plane, denoted by $p'e'$. In addition, e' denotes the intersection of line S_1S_2 and the right image plane I_2, called the epipole, and it is the common point of all the epipolar lines in the plane I_2. As *P* is a point in the 3D curve, *C*, the point p' must be on the extracted curve, C', in the right image. That means that the corresponding point of *p* in the left image should be the intersection of epipolar line $p'e'$ and curve C' in the right image. Using this method, the corresponding points of the two corresponding curves in the two images can be calculated.

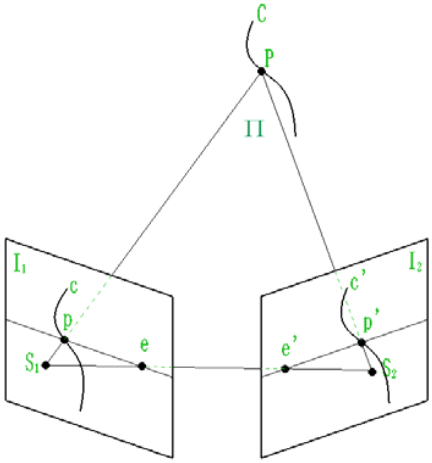

Fig. 5. Schematic principle of the epipolar line method

Furthermore, according to the calibration of the stereo vision, the coordinates of the 3D points on the reconstructed 3D curve can be obtained by using the triangular method.

After reconstructing the 3D curve, an effective method to find the accurate diameter of the hole is presented. When the axis of the 3D round hole is parallel to the *Z* axis, the projection on the *XY* plane of the reconstructed 3D curve should be a circle. Fig. 6 shows the projection on the *XY* plane of a 3D curve. P_1P_2 is the axis of the 3D round hole. *C* is the intersection curve of the hole and a curved surface. C' is the projection on the *XY* plane of the 3D curve *C*.

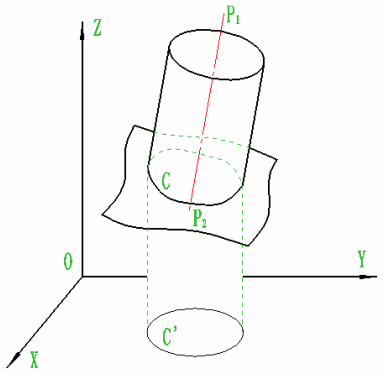

Fig. 6 The projection of a 3D curve on a curved surface

According to the angle relationship between the axis P_1P_2 and Z axis, which is determined by the fixture, the reconstructed 3D curve can be rotated to make its axis parallel to the *Z* axis by

$$\begin{bmatrix} x_i' \\ y_i' \\ z_i' \end{bmatrix} = Rot(X,\varphi)Rot(Y,\theta)\left(\begin{bmatrix} x_i \\ y_i \\ z_i \end{bmatrix} - \begin{bmatrix} x_c \\ y_c \\ z_c \end{bmatrix}\right), \tag{10}$$

and

$$\begin{bmatrix} x_c \\ y_c \\ z_c \end{bmatrix} = \left[\frac{1}{n}\sum_{i=1}^{n} x_i \quad \frac{1}{n}\sum_{i=1}^{n} y_i \quad \frac{1}{n}\sum_{i=1}^{n} z_i\right]^T, \tag{11}$$

where (x_i, y_i, z_i) are the coordinates of the *ith* reconstructed 3D point. θ is the pitch angle between the axis q_1q_2 of the 3D hole and *Y* axis. φ is the yaw angle between the axis q_1q_2 and *X* axis. These angle parameters can be obtained according to the configuration of the clamping apparatus, CAD model of the parts and calibration of the stereo vision.

However, the errors of the provided angles θ and φ are often very large due to inaccurate fixation. Thus, an effective method to accurately adjust the pose of the 3D curve is presented to make its axis accurately parallel to the *Z* axis. It can be described by

$$\begin{bmatrix} x_i'' \\ y_i'' \\ z_i'' \end{bmatrix} = Rot(X,\Delta\varphi)Rot(Y,\Delta\theta)\begin{bmatrix} x_i' \\ y_i' \\ z_i' \end{bmatrix}, \tag{12}$$

where $\Delta\varphi$ and $\Delta\theta$ are the angle errors of φ and θ, respectively. Ignoring the high-order error terms, the transformation in equation (12) can be described by

$$\begin{bmatrix} x_i'' \\ y_i'' \\ z_i'' \end{bmatrix} \approx \begin{bmatrix} x_i' + \Delta\theta z_i' \\ y_i' - \Delta\varphi z_i' \\ z_i' - \Delta\theta x_i' + \Delta\varphi y_i' \end{bmatrix}. \quad (13)$$

Furthermore, an estimation function can be defined by

$$A = \frac{1}{n}\sum_{i=1}^{n}(D_i^2 - \overline{D^2})^2, \quad (14)$$

where, $D_i^2 = x_i''^2 + y_i''^2$, and $\overline{D^2} = \frac{1}{n}\sum_{i=1}^{n} D_i^2$.

Combining equations (13, 14) and ignoring the insignificant error terms, the estimation function can be described by

$$A = \frac{1}{n}\sum_{i=1}^{n}\left[a_i + 2b_i\Delta\theta + 2c_i\Delta\varphi\right]^2, \quad (15)$$

where

$$\begin{cases} a_i = x_i'^2 - \overline{x_i'^2} + y_i'^2 - \overline{y_i'^2} \\ b_i = x_i' z_i' - \overline{x_i' z_i'} \\ c_i = -y_i' z_i' + \overline{y_i' z_i'} \end{cases}, \quad (16)$$

As the conditions for function A to be minimum are $\partial A/\partial\Delta\theta = 0$ and $\partial A/\partial\Delta\varphi = 0$, according to equation (15), they can be described by

$$\begin{cases} \sum_{i=1}^{n} 2b_i\left[a_i + 2b_i\Delta\theta + 2c_i\Delta\varphi\right] = 0 \\ \sum_{i=1}^{n} 2c_i\left[a_i + 2b_i\Delta\theta + 2c_i\Delta\varphi\right] = 0 \end{cases}, \quad (17)$$

Then, the angle error $\Delta\varphi$ and $\Delta\theta$ can be easily obtained. Furthermore, adjusted by equation (13), the diameter of the 3D round hole can be calculated by

$$R = \frac{1}{n}\sum_{i=1}^{n}\sqrt{x_i''^2 + y_i''^2}, \quad (18)$$

V. Experimental Results

Fig. 7 shows the developed image acquisition system, which includes a co-axis light source, two CCDs, and a personal computer. The angle between the two lenses is $22°$. The maximum resolution of the CCD is 1200×1600 pixels. The stereo vision system is calibrated by a precise raster.

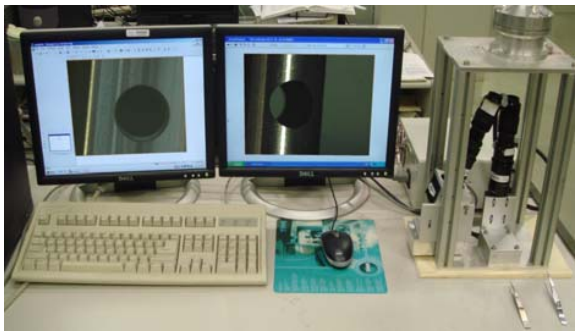

Fig. 7. The developed image acquisition system

To verify the effectiveness of the proposed method, the necessary experiments are conducted to measure a round hole in a cylindrical part. The main steps of the experiment are described as fellows.

Step 1: Acquire the image of the measured part using the developed stereo vision system;

Step 2: Calculate the gradient of the image, and build a virtual attraction field;

Step 3: Use a right octagon as the initial estimation of the desired curve in the image, and build a virtual beam chain;

Step 4: Calculate the displacement of all the virtual joints, and get the fitting beam chain at a certain scale;

Step 5: Decompose the obtained beam chain using $1/2^S$ scale, $S = 2, 3, ..., N$;

Step 6: Repeating step 4 and 5 for several times;

Step 7: Reconstruct the 3D curve using the epipolar line method and triangular method;

Step 8: Adjust the axis of the 3D round hole so that it is parallel to the *Z* axis, and calculate the average diameter of the curve projection on the *XY* plane;

In the following, the main experimental results of every step in the proposed method is given.

Fig. 8 shows the acquired gray images of a cylindrical part with a round hole. The first image (a) is acquired by the left CCD, and the second image (b) is acquired by the right CCD. In addition, every group of results is shown in the same order in Figs. 8-13.

Fig. 9 shows the initial positions of the virtual beam chains using right octagons in the gradient modulus of the two images, and the red arrows represent the virtual resultant force on the virtual joints. It also shows that there are large errors between the beam chains and the desired curve. Due to the surface texture of the part, the uneven light intensity, the background is complicated and the noise is large.

Fig. 10 shows the curve fitting results using the original beam chain at scale 1. Clearly, the proposed method can effectively drive the beam chain to fit the desired curves.

Repeating steps 5 and 4, the obtained virtual beam chains can be decomposed at smaller scales, and the desired curve can be re-fitted at a smaller scale by inheriting the fitting results of the previous scale. Fig. 11, 12 show the results of the virtual beam chains at scale $1/2$ and $1/2^3$, respectively. In the experiment, the fitting process at scale $1/2^2$ is skipped.

Fig. 13 shows the obtained final results of curve fitting at scale $1/2^3$ in the original gray images. The results prove that the virtual beam chains can exactly fit the desired curves.

Fig. 14 shows the reconstruction of the 3D points of the 3D curve. Some of these points on which the tangent is approximately parallel to the epipolar lines are ignored due to the large reconstruction errors.

According to equations (10-18), the diameter of the measured hole can be calculated with least squares error. The real average diameter of the hole is 4.024mm strictly measured by micrometer, and the measurement result using the presented method is 4.031 mm. The absolute measurement error is only 0.007mm, which meets most requirements of industrial

measurement for the parts.

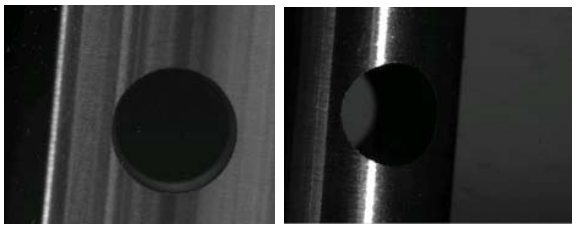

(a) (b)

Fig. 8 Acquired gray images of a cylindrical part

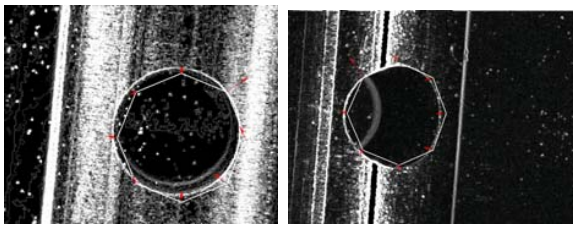

(a) (b)

Fig. 9 Initial positions of the virtual beam chains and the virtual resultant force on the virtual joints

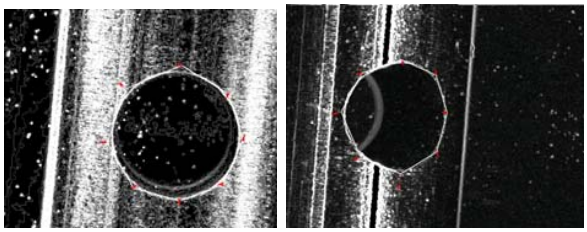

(a) (b)

Fig. 10 Fitting results of the virtual beam chains at scale 1

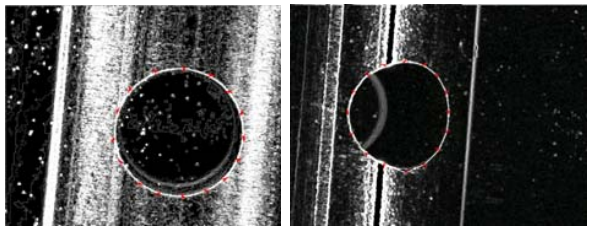

(a) (b)

Fig. 11 Fitting results of the virtual beam chains at scale $1/2$

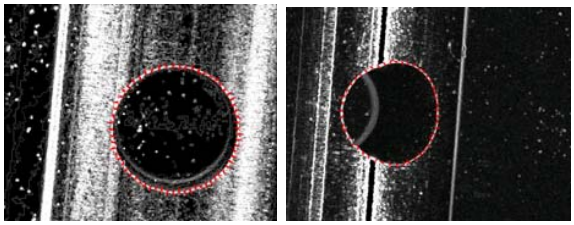

(a) (b)

Fig. 12 Fitting results of the virtual beam chains at scale $1/2^3$

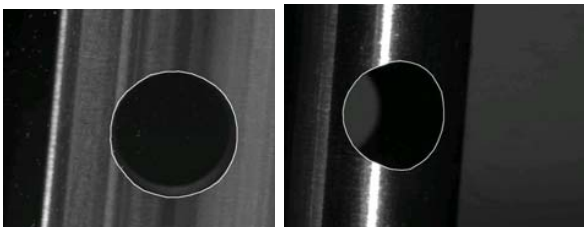

(a) (b)

Fig. 13 The final results of the curve fitting

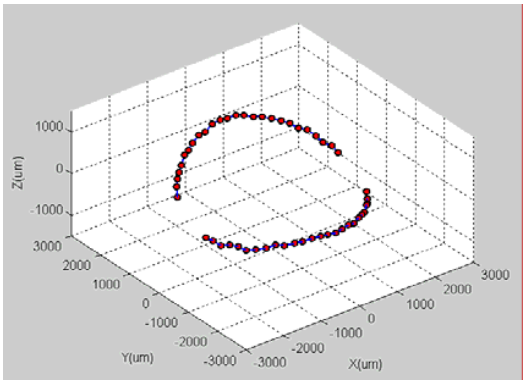

Fig. 15 The reconstructed points of the 3D curve

VI. Conclusion

This paper presents a method to reconstruct and measure 3D curves based on stereo vision. In this method, the curves in images can be represented by using a series of connected line segments, and every line segment can fit a section of the curve. To fit the desired curves in images, a virtual system including a virtual beam chain and a virtual attraction field is built. When the virtual beam chain is placed in the virtual attraction field, the beams can move towards the desired curve. When the equivalent resultant forces on the virtual joints reach zero, the curve can be fitted by the beam chain.

Due to the large errors in the installation of the measured part, the initial estimated positions of the beam chains are often far away from the desired curves. Therefore, a large scale of the beam chain can be used to fit the curve first. Then, the obtained beam chains are decomposed into smaller scales, and the curves are re-fitted by using the updated beam chains with the fitting results of the previous scale. Thus, the curve can be fitted with a high robustness at larger scales, and with a high accuracy at smaller scales. Furthermore, depending on the final positions of the beam chains in the two images, the measured 3D curve can be accurately reconstructed by using the epipolar line method. At last, using the proposed method, the axis of the 3D hole can be accurately adjusted so that it is parallel to Z axis, and the average diameter also can be accurately calculated.

In the experiments, a 3D round hole through a small cylindrical part is measured. The results show that the proposed method can effectively fit the desired curves in complicated backgrounds from coarse to fine, and the 3D curve can also be accurately reconstructed and measured. The

experimental results demonstrated that the presented method can reconstruct and measure 3D curves with acceptable errors, and can meet the industrial requirements of measurement.

ACKNOWLEDGMENTS

The work described in the paper was supported by the Research Grants Council of Hong Kong (RGC, No. 610708).

REFERENCES

[1] C. Y. Lin, A New Approach to Automatic Reconstruction of a 3-D World Using Active Stereo Vision. Computer Vision and Image Understanding, 2002. 85(2): p. 117–143.

[2] S Pollard and J Porrill, Robust recovery of 3D ellipse data. Brrtish Machine Vision Conf, 1992: p. 39-48.

[3] A. Wozniak and M. Dobosz, Factors Influencing Probing Accuracy of a Coordinate Measuring Machine. IEEE Transactions on Instrumentation and Measurement, 2005. 54(6).

[4] H. Shimotahira, K.I., S. C. Chu, C. Wah, F. Costen, and Y. Yoshikuni, Three-dimensional laser microvision. Applied Optics, 2001. 40(11): p. 1784-1794.

[5] S. Komatsu, H.S., and H. Ohzu, Laser scanning microscope with a differential heterodyne optical probe. Applied Optics, 1990. 29(28): p. 4244-4249.

[6] Z. Y. Wang, H.D., S. Park, and H. M. Xie, Three-dimensional shape measurement with a fast and accurate approach. Applied Optics, 2009. 48(6).

[7] R. Anchini, C.L., V. Paciello, and A. Paolillo, A Comparison Between Stereo-Vision Techniques for the Reconstruction of 3-D Coordinates of Objects. IEEE Transactions on Instrumentation and Measurement, 2006. 55(5).

[8] R. O. Duda and P. E. Hart, Use of the Hough Transform to detect lines and curves in pictures. Communications of the ACM, 1972. 15(1).

[9] A Leonardis and R Bajcsy, Finding parametric curves in an image. Second European Conf. Computer Visron,, 1992: p. 653-657.

[10] A. Albano, Representation of digitised contours in terms of conic arcs and straight line segments. Computer Graphics and Image Processing, 1974. 5: p. 23-33.

[11] Y Nakagawa and A Rosenfeld, A note on polygonal and elliptical approximation of mechanical parts. Pattern Recognition, 1979. 11: p. 133-142.

[12] Pavlidis, T., Curve fitting with conic splines. ACM Trans Graphics,, 1983. 2(1): p. 1-31.

[13] P.L. Rosin, G.A.W.W., Nonparametric Segmentation of Curves into Various Representations. IEEE Transactions on Pattern Analysis and Machine Intelligence 1995. 17(12): p. 1140-1153.

[14] Y-Z Liao, A two-stage method of fitting conic arcs and straight line segments to digitised contours. Conf. Pattern Recognition and Image Processing, 1981: p. 224-229.

[15] I. Weiss, Line Fitting in a Noisy Image. IEEE Transaction on Pattern Analysis and Machine Intelligence, 1989. 2(3).

[16] H. Qjidaa and L. Radouane, Robust Line Fitting in a Noisy Image by the Method of Moments. IEEE Transaction on Pattern Analysis and Machine Intelligence, 1999. 21(11).

[17] S. H. Park, K.M.L., and S. U. Lee, A Line Feature Matching Technique Based on an Eigenvector Approach. Computer Vision and Image Understanding, 2000. 77(3): p. 263–283.

[18] H. H. Joon, S.P.J., Contour Matching Using Epipolar Geometry. IEEE Trans. on Pattern Anal. Machine Intell., 2000. 22(4).